An entropic understanding of flow maldistribution in thermally isolated parallel channels

Toochukwu Aka, Shankar Narayan*
Department of Mechanical, Aerospace, and Nuclear Engineering, Rensselaer Polytechnic Institute, 110
8th Street, Troy, NY 12180
*Corresponding Author: narays5@rpi.edu

ABSTRACT

1

2

3

4

5

6

7

8

9

10

11

12

13

14

15

16

17

18

19

20

21

22

23

Flow across heated parallel channel systems exists in many applications. The performance of such systems experiencing multiphase flow could suffer from the deleterious effects of flow nonuniformity or maldistribution. Modeling the behavior of such systems is challenging due to the inherent non-linearity associated with the multiphase flow and the difficulty in determining the actual flow among several possible flow distributions. This study addresses the challenge by analyzing the entropy production in such systems. Using experiments on two thermally isolated, nominally identical, and externally heated parallel channels, we quantify irreversibility in the resulting multiphase flow by evaluating the entropy generation rate. Our experiments reveal that certain flow conditions result in severe maldistribution (flow ratio > 10) in the channels, associated with a sharp rise in entropy production. Such an increase is not predicted for uniform flow distribution across parallel channels, making maldistributed flow a thermodynamically favored state over equally distributed flow. We extend this understanding to non-identical parallel channels as well. With entropy analysis providing additional insight besides the fundamental equations governing mass, momentum, and energy conservation, this approach is valuable in predicting and controlling flow distribution in parallel channel systems.

Keywords: Parallel channels; flow distribution; entropy analysis; maldistribution; flow boiling.

1 Introduction

24

25

26

27

28

29

30

31

32

33

34

35

36

37

38

39

40

41

42

43

44

45

46

Parallel channels can scale performance in several engineering systems and devices, such as heat exchangers, chemical reactors, electronic cooling and power generation systems, fluidized beds, microfluidic devices, and fuel cells [1]–[6]. Under certain operating conditions, such systems face the risk of instability, wherein flow distribution between parallel channels becomes severely nonuniform. This phenomenon could occur even for parallel channels that are nominally identical. It is undesirable since it can reduce the system's performance and sometimes cause irreversible damage [1][2]. Therefore, prior efforts have focused on the prediction and characterization of flow maldistribution in parallel channels, especially where multiple phases (liquid and vapor) coexist [2], [3], [7]–[11]. Taitel et al. [10] showed that symmetrical heating of a multi-channel system can be unstable and established a control procedure against flow maldistribution. Minzer et al. [12] used linear stability analysis to differentiate between stable and unstable flow solutions. Results from Minzer's study show that flow distribution may depend on history. Yang et al. [13] developed a 3D computational model of a nine parallel-channel system and showed that under the same conditions, the flow tends to be more equally distributed in parallel channels with a circular crosssection when compared to a triangular cross-section. With the aid of a model, Zhang et al. [7] showed that flow distribution in a parallel channel can be controlled by manipulating the total flow rate if the parallel channels are distinct. Natan et al. [14] showed up to five obtained for a single flow rate through a two parallel-channel system and speculated that the most feasible solution is the one with the least pressure drop. In these studies, the methodology employed in predicting the stability of different flow distributions involves the perturbation of the Navier Stokes' equations [7], [10], [12], which

establishes a criterion to ascertain if maldistribution can occur or not. While this approach

distinguishes between stable and unstable flows [9], [12] it is unclear why a particular flow distribution is bound to occur over other mechanically feasible possibilities. We address this gap in knowledge by introducing thermodynamic considerations to flow distribution in parallel channels.

47

48

49

50

51

52

53

54

55

56

57

58

59

60

61

62

63

64

65

66

67

68

69

Entropy analysis, based on the second law of thermodynamics, is a valuable tool for analyzing the directionality of processes in physical systems. Entropy analysis evaluates and optimizes thermalhydraulic systems by quantifying the degree of irreversibility associated with flow and energy transfer in systems. A recent study applied multiscale entropy analysis in identifying flow regimes and dynamic characteristics of gas-liquid two-phase flows in horizontal channels [15]. Several studies have also focused on optimizing heat exchangers via entropy generation minimization [16] - [19]. Applying entropy analysis to a known phenomenon, Zupanovic et al. [20] showed that Kirchoff's loop law can be derived from the maximum entropy principle. Concerning stationary two-phase flow distribution, Giannetti et al. [21] developed a variational formulation of two-phase flow distribution at a fluid junction. They showed that the predicted flow distribution can correspond to different entropy production rates depending on the chosen two-phase flow model. For example, their study showed that the homogeneous model leads to a higher entropy production rate than the separated flow model. The study showed that the extremisation of the entropy generation rate provides the additional conditions necessary for closing the problem formulation to model flow distribution in fluid networks. This study uses entropy analysis to show the relationship between entropy generation and flow distribution in a system consisting of two thermally isolated parallel channels. In this case, externally heated channels cause vaporization and multiphase (liquid-vapor) flow. This study provides, for the first time, a thermodynamic perspective on flow distribution in parallel channels in such conditions. We demonstrate how the

entropy analysis can be applied to distinguish between stable and unstable flow states corresponding to the same system operating conditions.

2 FLOW DISTRIBUTION IN PARALLEL CHANNELS

72

79

The changes in flow properties like pressure and temperature across parallel channels are useful in quantifying the flow performance. For given inlet conditions, such as inlet pressure P_i and temperature T_i , the exit properties like pressure P_e and enthalpy h_e can be calculated using the equations for conservation of mass, momentum balance, and the first law of thermodynamics. These fundamental equations take the following form for two thermally isolated parallel channels sharing a common inlet and exit (Figure 1) and operating at steady-state.



Figure 1. Two thermally isolated parallel channels sharing a common inlet and exit.

$$\int_{CS} \rho \bar{v} \cdot d\bar{A} = 0 \tag{1}$$

82
$$\int_{CS} \bar{v} \rho \bar{v} \cdot d\bar{A} = \int_{CS} -p \ d\bar{A} + \int_{CS} \bar{\bar{\tau}} \ d\bar{A} + \int_{CS} \bar{g} \ dV$$
 (2)

- Here \bar{v} , p, $\bar{\bar{\tau}}$, and \bar{g} denote velocity, pressure, tangential stress, and body force per unit volume,
- 84 respectively. In addition, the first law of thermodynamics gives

$$\int_{CS} h \rho \bar{v} \cdot d\bar{A} = \int_{CS} d\dot{Q} \tag{3}$$

Application of these fundamental equations to flow in individual channels allows predicting the pressure change, $\Delta P = P_i - P_e$ for different flow rates, \dot{m} . The model outcome could suggest

multiple possible flow distributions for a simple case involving two nominally identical channels (Figure 1), where the flow is heated as it passes through them. For example, one possible model prediction can be equally distributed flow for all possible channel flow rates, irrespective of the exit quality (Figure 2, distribution 1). Another possibility is that the flow is liquid and equally distributed at high flow rates, whereas it becomes unequally distributed or maldistributed with flow boiling at low flow rates (Figure 2, distribution 2). A fundamental aspect that is still unclear is which of the two distributions is likely to occur and why.

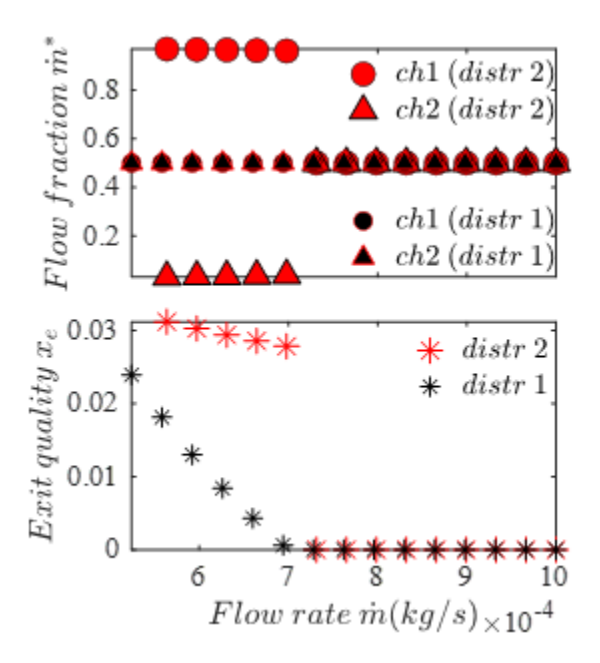


Figure 2. Possible flow distribution predictions in two parallel channels (fluid: water, diameter: 1.4 mm, length: 0.3 m).

Previous studies have used a criterion based on the perturbation of the momentum balance equation to distinguish between stable (feasible) and unstable (infeasible) flow distributions. For example, based on this criterion, the stable distribution for the above system has been predicted as a maldistributed flow rather than a uniformly distributed one. While this prediction may be accurate, the criterion provides no reason why a maldistributed state is more stable than equally distributed

flow when both distributions satisfy the basic equations governing mass, momentum, and energy conservation. Moreover, the number of viable flow distributions increases with the number of parallel channels, making the traditional modeling approach more challenging – hence, a clearer understanding of the maldistribution phenomenon is necessary.

The challenge introduced by non-unique solutions can be addressed by considering the entropic aspects of flow, which is often overlooked. Internal flow with energy transfer is associated with entropy generation as flows occur from the inlet i to the exit e of a channel. For steady flow through boundary-heated channels, the total entropy generation rate, \dot{S}_{gen} can be calculated using the entropy balance equation for an open system.

$$\int_{CS} s\rho \bar{v} \cdot d\bar{A} = \int_{CS} \frac{d\dot{Q}}{T_w} + \dot{S}_{gen} \tag{4}$$

Here \dot{Q} denotes net heat transferred from the boundary into each channel maintained at a uniform temperature of T_w . The increase in entropy is also caused by the irreversibility associated with flow in the channels, \dot{S}_{gen} . Irreversibility occurs in this pressure-driven flow due to many reasons, including heat transfer across a finite temperature difference, friction between the fluid and the channel wall, sudden changes in configuration and direction of flow, and the mixing of thermally dissimilar fluids from parallel channels at the flow junctions or headers [22]. The second law of thermodynamics requires that the rate of entropy generation, $\dot{S}_{gen} \geq 0$, wherein equality holds only if the process is internally reversible. We believe that the flow distribution in a multi-channel network is governed by the maximization of \dot{S}_{gen} . This study investigates entropy production in model-predicted flow distributions in parallel channels. With the help of experiments involving

thermally isolated parallel channels, we show how the entropy analysis determines the thermodynamically preferred flow distribution, which matches our observations.

3 EXPERIMENTAL PROCEDURE

123

124

125

126

127

128

129

130

131

132

133

134

135

136

137

138

139

140

141

142

143

144

The test section (Figure 3) comprises two parallel channels with a shared inlet and exit. Each channel consists of a valve to control flow, a flowmeter (Omega FLR-1008ST, ±3.3 × 10^{-5} kg/s), and channels made of stainless steel capillary tubes of internal diameter 1.4 mm, outer diameter 3.18 mm and length 305 mm, circumferentially interfaced with heaters (125 W) and fiberglass insulation. Also, pressure sensors (Omega PX309-030A5V, ±0.52kPa) and thermocouples (Omega T-type, ±1°C) were positioned at the inlet and exit of the test section to monitor flow. Four additional temperature sensors were attached to each channel wall at equidistant positions to keep track of the channel wall temperature. Other components in the testbed include a temperature-controlled heated tank as a liquid reservoir, a chiller to extract heat from the working fluid, an electronic valve, and a gear pump (Micropump, GA-X21.CFS.E, 0 – 65 Hz) to maintain stable two-phase flow in the channels. The parallel channels are independently heated using programmable DC power supply modules (BK Precision, XLN 15010, $\pm 0.01\%$). The testbed uses water, and the system was maintained within a pressure range of 8 to 33kPa. In addition to the flowmeters keeping track of the flow rate in each channel of the test section, a flow meter is positioned after the pump to monitor the total flow rate. Including this flow meter also allows for estimating the flow rate in the channel with minimal flow during severe flow maldistribution.

In order to improve baseline stability, ensure consistency, and maintain the required pressure at the start of an experiment, the setup is initially de-aerated, and the fluid tank is heated before turning on the pump. This step ensures that the working fluid instantaneously gets to the pump at startup, preventing cavitation and potential damage to the pump. Experiments typically involve liquid flow in sequence from the pump to the test section, storage tank, and chiller. Within the test section, fluid may split between two parallel channels, or flow might be limited to a single channel if the valve on the other branch is fully shut. Experiments typically involve liquid entering the test section below saturation conditions and exiting as liquid, liquid vapor mixture, or super-heated vapor.

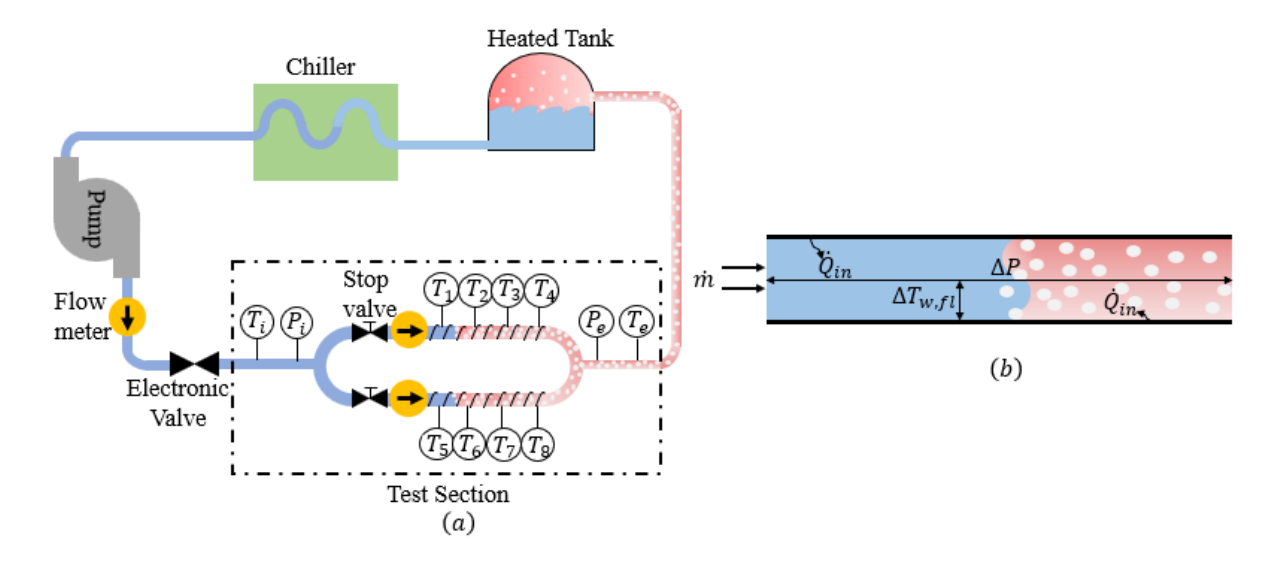


Figure 3. (a) Experimental pumped liquid cooling cycle. (b) Illustration of flow in a single channel.

Initial experiments involve thermal characterization of each channel to determine the relationship between readily available physical quantities (mass flow rate \dot{m} , channel surface area A_s and temperature difference between the channel wall and ambient $T_w - T_\infty$) and heat loss \dot{Q}_{loss} to the surroundings, as shown in Figure 4. Therefore, for a given electrical heat load $\dot{Q}_h = IV$, the net heat transfer to the fluid $\dot{Q} = \dot{Q}_h - \dot{Q}_{loss}$, where $\dot{Q}_{loss} = \dot{Q}_{loss}(\dot{m}, A_s, T_w - T_\infty)$ can be estimated from Figure 4. This step is useful, especially when \dot{Q} cannot be directly obtained using mass, temperature, and pressure measurements of the liquid-vapor mixture flow. An interface designed

with LABVIEW and MATLAB is used for automated actuator control besides recording, compiling and plotting the experimental data from the testbed.

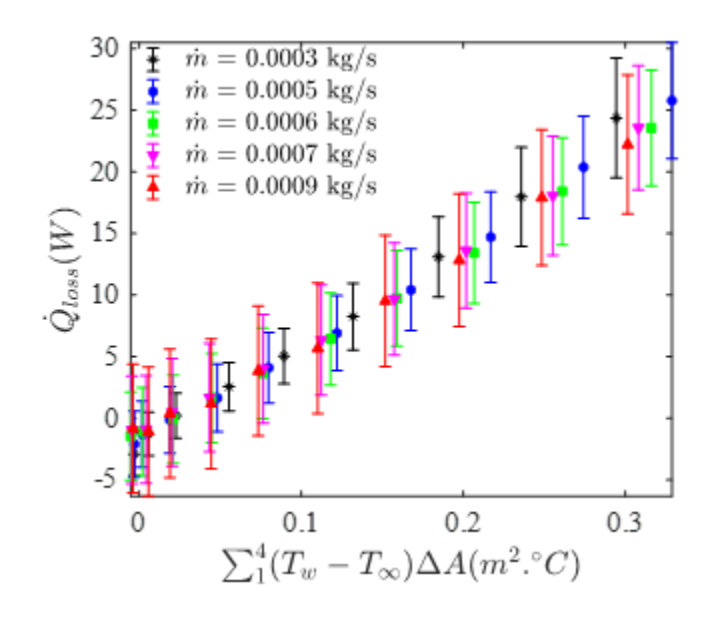


Figure 4. Heat loss characterization of a single channel

The uncertainty in a parameter *f* is determined by applying the propagation of error [23]–[25], as shown in Eq. 5,

167
$$\Delta f = \sqrt{\left(\frac{\partial f}{\partial x_1} \Delta x_1\right)^2 + \left(\frac{\partial f}{\partial x_2} \Delta x_2\right)^2 + \dots + \left(\frac{\partial f}{\partial x_n} \Delta x_n\right)^2}$$
 (5)

where $\Delta x_1 \dots \Delta x_n$ are the errors associated with the measurement of n independent variables, $x_1 \dots x_n$ to calculate the parameter f.

4 ENTROPY GENERATION AND SOURCES OF IRREVERSIBILITY

163

164

170

The following equations describe the first and second laws of thermodynamics for the N-channel system, which allow for determining \dot{S}_{gen} .

173
$$\dot{m}(h_i - h_e) = \sum_{j=1}^{N} \dot{Q}_{h,j} - \dot{Q}_{loss,j}$$
 (6)

174
$$\dot{S}_{gen} = \dot{m} \left(s_e(P_e, h_e) - s_i(P_i, T_i) \right) - \sum_{j=1}^{N} \frac{\dot{Q}_{h,j} - \dot{Q}_{loss,j}}{T_{w,j}}$$
 (7)

The specific entropies at the inlet (s_i) and outlet (s_e) of the channel assembly are functions of inlet pressure P_i and temperature T_i , and exit pressure P_e and specific enthalpy, h_e , respectively. Here \dot{Q} is obtained from the difference between the electrical heat load $\dot{Q}_{h,j}$ and heat loss $\dot{Q}_{\infty,j}$ in each channel j. In a system of parallel channels, the total rate of entropy generated consists of the rate of entropy generated within each channel member $\dot{S}_{gen,j}$, the rate of entropy generated from the splitting of flow at the common inlet $\dot{S}_{gen,split}$ and the rate of entropy generated at the common exit from irreversible heat transfer within mixing fluid streams $\dot{S}_{gen,mix}$. Compared with other contributions, $\dot{S}_{gen,split}$ is negligible because of the insignificant change in the thermodynamic properties of the fluid during the splitting process. As a result, \dot{S}_{gen} is expressed as

184
$$\dot{S}_{gen} = \dot{S}_{gen,mix} + \sum_{j=1}^{N} \dot{S}_{gen,j}$$
 (8)

Since the channel assembly is thermally insulated and the mixing process is relatively fast, adiabatic conditions are assumed in determining $\dot{S}_{gen,mix}$.

$$\dot{S}_{gen,mix} = \dot{m}s_{mix}(P_{mix}, h_{mix}) - \sum_{j=1}^{N} \dot{m}_{j}s_{e,j}$$
 (9)

Where the specific entropy of the fluid mixture at the exit (s_{mix}) is a function of the mixture pressure P_{mix} and enthalpy h_{mix} . In parallel channel experiments, P_{mix} and h_{mix} are typically P_e and h_e , respectively. However, in cases where single-channel experiments are used to estimate the properties of flow in parallel channels, P_{mix} and h_{mix} are given as

$$h_{mix} = \sum_{j=1}^{N} \dot{m}_{j}^{*} h_{e,j}, \qquad (10)$$

193
$$P_{mix} = \sum_{j=1}^{N} \dot{m}_{j}^{*} P_{e,j}. \tag{11}$$

194 4.1 Sources of Irreversibility in a Single Channel

195

196

197

198

199

200

201

202

Besides other sources, the hydraulic and thermal resistance affecting the flow and heat transfer in the two channels contribute significantly to irreversibility. The pressure drop $\Delta P = P_i - P_e$ across the channel depends on the flow rate and the hydraulic resistance to flow, which depends on fluid friction. Hence, ΔP indicates how certain flow aspects (e.g., friction) introduce irreversibility in the system. Similarly, heat transfer from the wall at T_w to the fluid at T_f is an irreversible process requiring a temperature differential $T_w = T_f$. However, for an internally-reversible heat transfer process $S_{gen} = T_{gen} = T_{gen}$

$$T_{rev} = \frac{\dot{Q}_h - \dot{Q}_{loss}}{\dot{m}(s(P_i, h_e) - s(P_i, T_i))}$$
(12)

In practice, the channel wall temperature (T_w) is much larger than T_{rev} due to irreversibilities. Hence, $\Delta T_w = T_w - T_{rev}$ is used as an indirect measure of deviation from an ideal heat transfer process. Figure 5a shows ΔP , ΔT_w , the exit vapor quality x_e , and the entropy generation rate \dot{S}_{gen} for a single channel heated at $\dot{Q}_h = 70$ W.

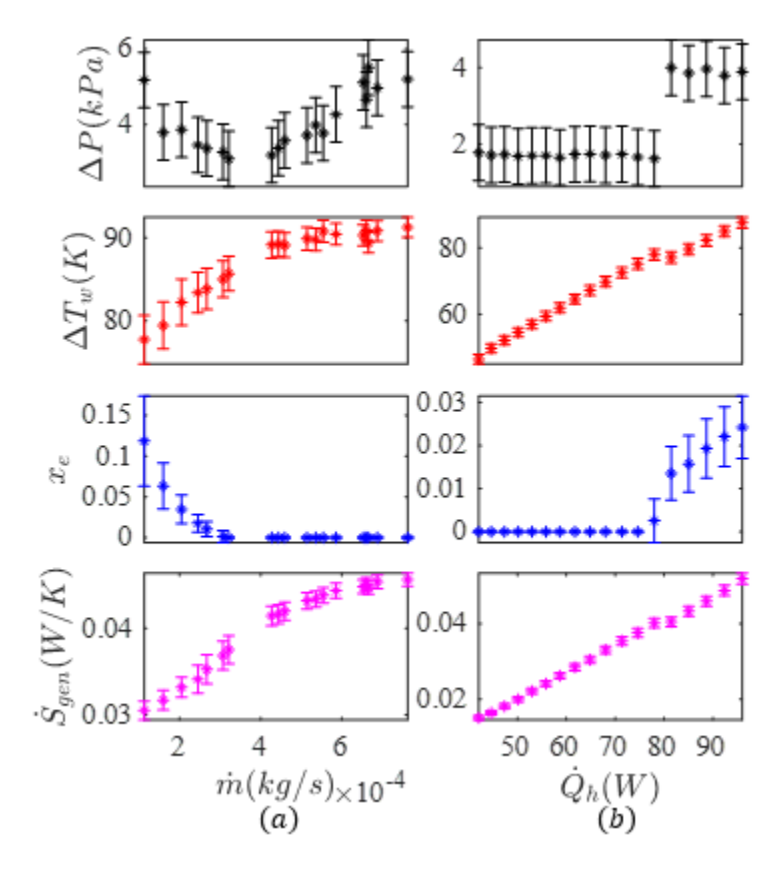


Figure 5. Variation of single-channel pressure drop ΔP , the wall temperature difference ΔT_w , exit quality x_e , and entropy generation \dot{S}_{gen} , as a function of (a) flow rate \dot{m} at $\dot{Q}_h = 70$ W. (b) external heat load \dot{Q}_h at $\dot{m} = 3.48 \times 10^{-4}$ kg/s.

Starting from a large flow rate, a continuous decrease in \dot{m} results in liquid-to-vapor phase change. Consequently, the fluid phase at the exit changes from liquid ($x_e = 0$) to a liquid-vapor mixture ($x_e > 0$). With boiling and an increase in vapor production, heat transfer characteristics within the channel change to become more efficient, which can be seen in the lowering of ΔT_w with an increasing x_e . Correspondingly, the rate of entropy generation also decreases. This decrease in \dot{S}_{gen} occurs despite increasing ΔP , which indicates the more significant role of heat transfer

irreversibility over flow non-idealities. At large flow rates, when ΔT_w does not change much with an increase in \dot{m} , \dot{S}_{gen} increases mainly due to rising ΔP – a regime where flow non-idealities dominate.

To further investigate the contribution of flow and heat transfer irreversibilities to the total entropy production, we also varied channel heating rates (\dot{Q}_h) while keeping the flow rate (\dot{m}) constant. Figure 5b shows the variation of ΔP , ΔT_w , the exit vapor quality (x_e) , and the entropy generation rate \dot{S}_{gen} for a single channel with \dot{Q}_h at a constant $\dot{m}=3.48\times 10^{-4}{\rm kg/s}$. Starting from a small heat load, a continuous increase in \dot{Q}_h results in the phase change from liquid $(x_e=0)$ to liquid-vapor mixture $(x_e>0)$, a jump in ΔP and an increase in both ΔT_w and \dot{S}_{gen} . The sudden increase in ΔP is due to vapor production (phase change) in the channel at the threshold value of the heating rate around 80 W. The increase in ΔT_w and \dot{S}_{gen} with no significant change in ΔP before and after phase change indicates that the irreversibilities associated with heat transfer contribute more to \dot{S}_{gen} than the flow irreversibilities.

4.2 Irreversibility in two thermally isolated Parallel Channels

Unlike flow in a single channel, entropy generation rates in two parallel channels are also influenced by the nature of the flow distribution. Flow distribution is quantified in terms of \dot{m}^* which denotes the flow fraction in a channel relative to the total flow rate. Flow distribution is obtained based on measured flow rates, $\dot{m}_1^* = \dot{m}_1/(\dot{m}_1 + \dot{m}_2)$ and $\dot{m}_2^* = \dot{m}_2/(\dot{m}_1 + \dot{m}_2)$. For instance, $\dot{m}^* = 0.5$ denotes equally distributed flow in a two-channel system. Figure 6 shows the observed flow fraction \dot{m}^* , total entropy generation \dot{S}_{gen} , pressure drop ΔP , and the temperature difference ΔT_w for different total flow rates \dot{m} in two nominally-identical thermally-isolated parallel channels under a constant heat load of 70 W each.

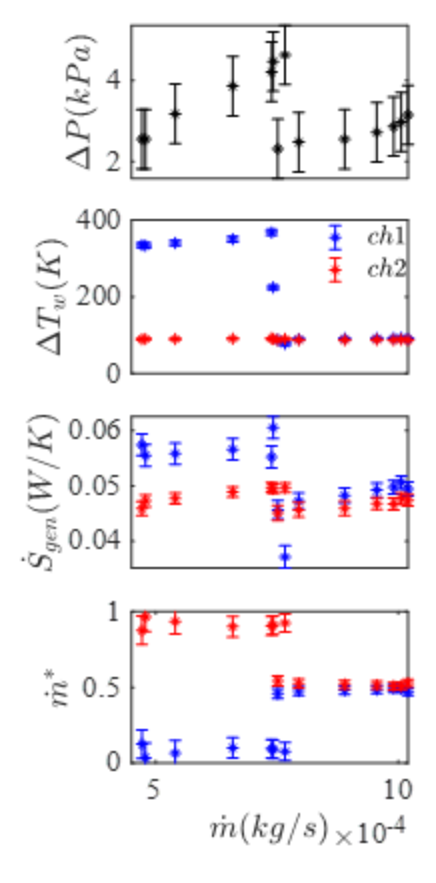


Figure 6. Variation of parallel channel pressure drop ΔP , wall temperature difference ΔT_w , entropy generation \dot{S}_{gen} , and flow fraction \dot{m}^* as a function of the flow rate \dot{m} at $\dot{Q}_h = 70 \text{ W}$

At high flow rates in the two parallel identical channels, the pressure difference (ΔP) decreases as the total flow rate (\dot{m}) decreases. For a large \dot{m} , the fluid emerges as a liquid at the exit. Since the characteristics of heat transfer do not change much under these conditions, there is no significant change in the temperature difference, ΔT_w . Hence, like flow in a single channel, the \dot{S}_{gen} in each channel, and the ΔP across the channel decreases as \dot{m} decreases and ΔT_w is expectedly uniform. As \dot{m} decreases further, the fluid at the exit transitions from liquid to a liquid-vapor mixture due to heat-induced boiling. Phase-change characteristics now initiate severe flow maldistribution, as indicated by the departure in \dot{m}^* for the channels. This uneven distribution occurs with a sudden decrease in \dot{m}^* for channel 1 and an increase in \dot{m}^* for channel 2. A sudden rise in ΔP across the

252 channels is also observed. The decrease in \dot{m} also results in a sharp rise in ΔT_w and \dot{S}_{gen} in channel 253 1. In comparison, the change in \dot{S}_{gen} is not that significant and ΔT_w is mostly invariant in channel 254 2.

The relative effects of flow and heat transfer irreversibilities on \dot{S}_{gen} depend on the system. In this case, when the flow was equally distributed or when it remained maldistributed, the variation in \dot{S}_{gen} is due to hydraulic irreversibilities. However, in this case, the transition from uniform to non-uniform flow distribution was mainly due to thermal irreversibilities. Considering both channels collectively, there is an increase in the total \dot{S}_{gen} . Hence, an important conclusion from this observation is that severe flow maldistribution is associated with a sharp rise in entropy production. The following section describes why severe maldistributed flows prevail over uniform and moderately non-uniform flows.

5 Entropy Generation and Flow Distribution in Thermally Isolated Parallel Channels

Although the flow rate in a single channel can be predicted based on the pressure drop and the channel geometry [1], the possible flow distributions in parallel channels are multiple and not easily predictable. This section shows why severely maldistributed flow prevails over uniform and moderately non-uniform distribution by considering the two parallel channels. Here, we compare the entropy generation in an actual flow distribution with the entropy generation if the flow were to have an unstable flow distribution. The "coupled" experiments involving simultaneous flow in both channels determine the flow distribution in the parallel channel assembly (Figure 7a). However, estimating the characteristics of unstable flow distributions for the same conditions used for the "coupled" experiments is not as straightforward since they do not occur naturally.

Therefore, each channel is tested individually by disconnecting the other channel from the system by shutting off the corresponding upstream valve, as illustrated in Figure 7b. Hence, such experiments are called "uncoupled." The unstable flow characteristics of the parallel channel system, such as flow distribution, are determined using the characteristics observed in the uncoupled experiments. For instance, if flow rates \dot{m}_1 and \dot{m}_2 were observed in channels 1 and 2 for a pressure drop ΔP in the uncoupled experiments, we estimate the flow distribution in an equivalent parallel channel system (with pressure drop ΔP) as $\dot{m}_1^* = \frac{\dot{m}_1}{\dot{m}_1 + \dot{m}_2}$ and $\dot{m}_2^* = \frac{\dot{m}_2}{\dot{m}_1 + \dot{m}_2}$.

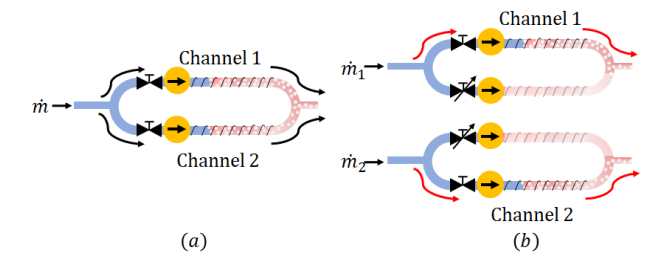


Figure 7. Illustration of (a) coupled and (b) uncoupled channels 1 and 2.

5.1 Flow in Parallel Channels under Uniform Operating Conditions

Figure 8 compares the entropy generation rates for severely maldistributed and uniformly distributed flows. In order to calculate the entropy production rates for maldistributed flow, the two channels are equally heated $(\dot{Q}_{h,1}=\dot{Q}_{h,2}=70~\text{W})$, and the total flow rate, \dot{m} is gradually reduced (Figure 8a). Alternatively, the total flow rate can be held fixed ($\dot{m}=6.96\times10^{-4}~\text{kg/s}$), and the heating rates, although uniform $(\dot{Q}_{h,1}=\dot{Q}_{h,2}=0.5\dot{Q}_h)$, can be gradually increased (Figure 8b). Then Eq. (7) is used to determine \dot{S}_{gen} using the measured inlet and exit flow properties and wall temperatures. The entropy generation rate and flow distributions from these experiments are indicated as "coupled" channels in Figure 8.

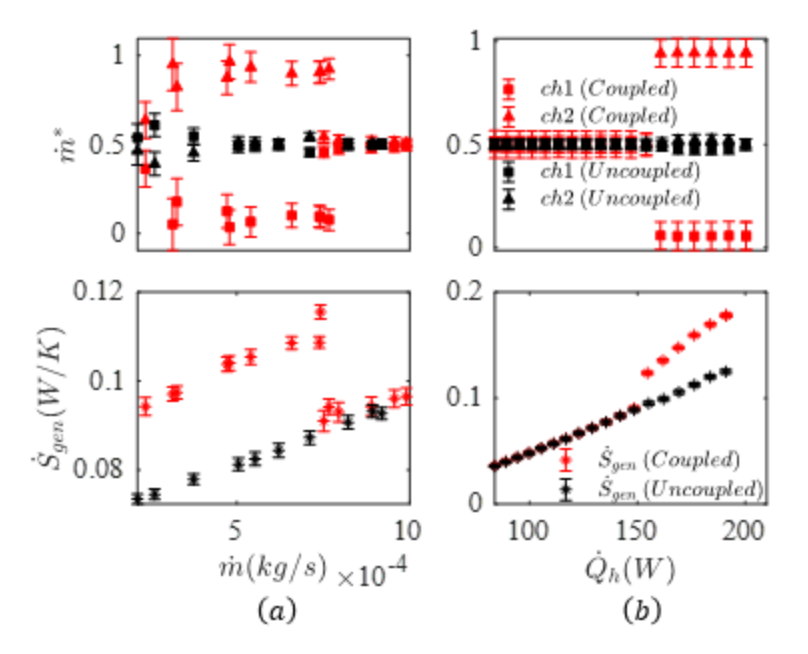


Figure 8. Variation of \dot{m}^* and \dot{S}_{gen} with \dot{m} for severely maldistributed and uniformly distributed flow for (a) varying \dot{m} with $\dot{Q}_{h1} = \dot{Q}_{h2} = 70 W$, and (b) varying \dot{Q}_h at $\dot{m} = 6.96 \times 10^{-4} \text{kg/s}$.

Uniformly distributed flow at all flow rates or heat loads may be expected because of the uniformity of physical conditions across both channels. To estimate the entropy generation rate for uniformly distributed flow in parallel channels, we individually test each channel in the testbed by isolating the other channel from the system using the valves shown in Figure 7b. Due to similar geometry and heating conditions, the total rate of entropy generation is obtained from Eq. 8 based on a common experimental input variable such as flow rate ($\dot{m}_1 = \dot{m}_2 = \dot{m}/2$) (Figure 8a) or heat load ($\dot{Q}_{h,1} = \dot{Q}_{h,2}$) (Figure 8b), yielding \dot{S}_{gen} corresponding to the hypothetical case of uniformly distributed flow ($m^* = 0.5$) in the parallel channel assembly. These results are shown as "uncoupled" channels in Figure 8.

Figure 8 compares \dot{S}_{gen} for maldistributed and uniformly distributed flow in the parallel channels. Figure 8a shows flow distribution and entropy generation when the flow rate \dot{m} is gradually decreased, while a steady heating power of 70 W is applied to both channels. Likewise, Figure 8b

shows the flow distribution and entropy production when the heating load, although the same for both channels, is gradually increased with a total flow rate fixed at $\dot{m} = 6.96 \times 10^{-4}$ kg/s. In case of single channel experiments, the flow rate in each channel is halved with $\dot{m} = 3.48 \times 10^{-4} \, \text{kg/s}$. When \dot{m} is large or \dot{Q}_h is low, the flow is equally distributed between the channels. For these conditions, \dot{S}_{gen} decreases with \dot{m} (Figure 8a) and increases with \dot{Q}_h (Figure 8b). However, as \dot{m} decreases or \dot{Q}_h increases, the flow eventually becomes severely maldistributed. Evidently, this maldistribution corresponds to a sudden jump in \dot{S}_{gen} . However, if the channels experience uniform flow, then \dot{S}_{gen} does not show any dramatic variation. For these conditions representing a hypothetical uniform flow case, \dot{S}_{gen} continues to decrease with \dot{m} and increase with \dot{Q}_h . Figure 8 shows that the entropy generation rate of severely maldistributed flow is much greater than equally distributed flow under similar conditions. Hence, flow maldistribution seen here is thermodynamically more favorable over equally distributed flow. It is due to this reason that nonuniform flows are sustained unless conditions are significantly altered to enable uniform flow distribution.

5.2 Flow in Parallel Channels under Non-uniform Conditions

307

308

309

310

311

312

313

314

315

316

317

318

319

320

321

322

323

324

325

326

327

Severe maldistribution also occurs in parallel channels under non-uniform or dissimilar conditions, which can be explained using entropy analysis. To understand the effects of channel dissimilarity, we use different heat loads and valve openings associated with each channel to compare the entropy production rates. Figure 9 shows the flow behavior with $\dot{Q}_{h,1} = 80 \text{ W}$ and $\dot{Q}_{h,2} = 70 \text{ W}$, with the channel 1 valve fully open and the channel 2 valve half-opened. Since the channel conditions are inherently different, flow distribution is never uniform. Still, model predictions

could indicate multiple possibilities. For example, in this case, the predictions can indicate either marginal or significant muldistributions in these channels.

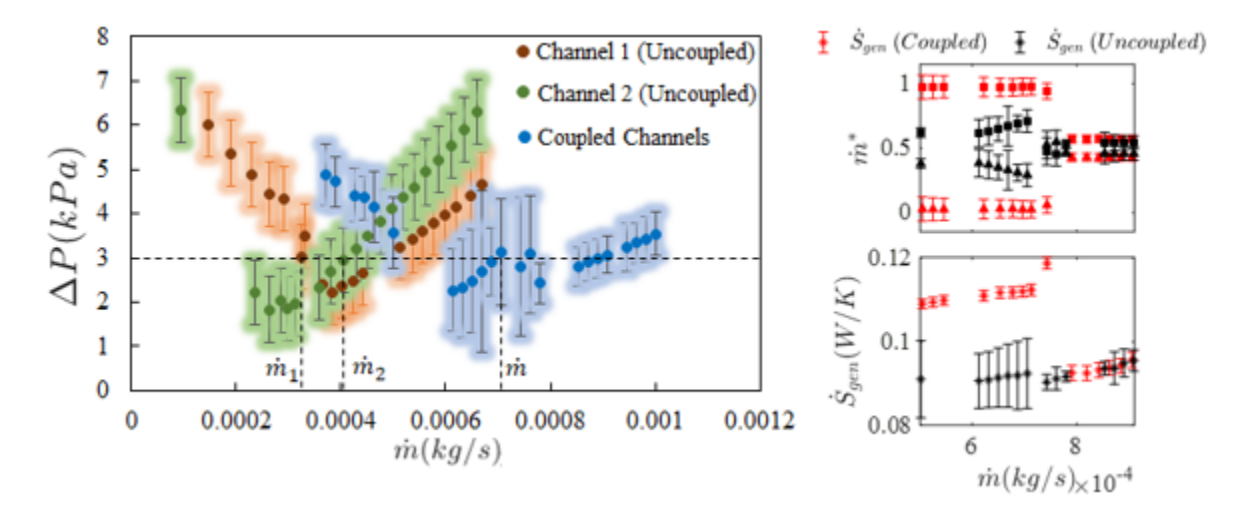


Figure 9. Variation of \dot{m}^* and \dot{S}_{gen} with \dot{m} for severely maldistributed and moderately maldistributed flow

When flow occurs in both channels simultaneously, the distribution (\dot{m}^*) is directly measured, and Eq. (7) is used to obtain \dot{S}_{gen} using the measured flow properties as described earlier. These results shown in Figure 9 (right) are indicated as coupled channels. In order to estimate other possible distributions, we use flow characteristics in individual (uncoupled) channels, with heating and valve settings similar to the coupled channels experiment. The flow characteristics, given by ΔP versus \dot{m} for the uncoupled and coupled channels, are shown in Figure 9 (left). For a total flow rate \dot{m} observed in the experiments, the flow distributions in uncoupled channels 1 (\dot{m}_1) and 2 (\dot{m}_2) are obtained such that $\dot{m}_1 + \dot{m}_2 = \dot{m}$, with flow rates \dot{m}_1 and \dot{m}_2 corresponding to the same pressure drop ΔP for the specific \dot{m} in the coupled experiments. To do this we find the intersection of a constant ΔP line with the ΔP versus \dot{m} characteristic curves for each channel, resulting in flow distribution \dot{m}_1^* and \dot{m}_2^* whose sum is unity. Mathematically, this can be expressed as a minimization problem with \dot{m}_1^* as the argument.

$$\dot{m}_{1}^{*} = \arg\min_{\dot{m}_{1}^{*} \in [0,1]} |\Delta P_{1}(\dot{m}_{1}^{*}) - \Delta P_{2}(1 - \dot{m}_{1}^{*})| \tag{13}$$

This procedure allows calculating \dot{m}_1^* , $\dot{m}_2^* = 1 - \dot{m}_1^*$ and the entropy generation, \dot{S}_{gen} using $\dot{S}_{gen,1}$ and $\dot{S}_{gen,2}$ from single-channel experiments and $\dot{S}_{gen,mix}$ to account for the adiabatic mixing of the two fluid streams in Eq. (8). In conclusion, the resulting flow distribution for uncoupled channels indicates a moderate maldistribution and the corresponding \dot{S}_{gen} is less than the coupled experiment.

Due to dissimilar valve openings and heating of the two channels, flow characteristics are expected to differ. For large values of \dot{m} , both uncoupled and coupled channel results indicate that the flow is slightly maldistributed mainly due to differences in channel valve opening and \dot{S}_{gen} decreases with \dot{m} . But as the total flow rate \dot{m} decreases further, both coupled and uncoupled channel results indicate larger flow maldistribution. Typical static modeling approaches could indicate that moderate maldistribution distribution is viable even for low total flow rates. However, an entropy analysis shows that the \dot{S}_{gen} corresponding to severely maldistributed flow is greater than the \dot{S}_{gen} corresponding to the moderately maldistributed flow. Consequently, the significantly maldistributed state is thermodynamically favored over moderately non-uniform flow, as seen in the experiments.

6 CONCLUSION

This study analyzes entropy production and its relationship with flow distribution in thermally isolated parallel channels with multiphase flow. Parallel channels with multiphase flow, even if nominally identical, can experience maldistribution or unequal flow distribution, which is undesirable in many applications. Since such systems are inherently nonlinear due to multiphase

flow characteristics, modeling and predicting this phenomenon is challenging and often results in multiple viable solutions. This study shows how an entropy analysis of flow in channels can overcome this modeling challenge. We hypothesize that flow maldistribution is governed by a thermodynamically favored state with maximum possible entropy production among the several flow possibilities identified by solving the fundamental equations governing mass, momentum, and energy conservation.

Using experiments, we identify two primary sources of irreversibilities associated with heat transfer and flow. Although both sources are present under all conditions, experiments show that flow irreversibilities, such as flow friction, affect entropy generation at higher flow rates. In contrast, thermal irreversibilities, such as non-isothermal heat transfer, tend to affect entropy generation more at lower flow rates and higher heat rates.

The flow distribution in parallel nominally identical channels is uniform for high flow rates, corresponding to little to no phase change. However, a transition to maldistribution occurs when the flow rate is reduced, or the heating rate is increased. The transition from uniform to non-uniform flow distribution corresponds to a sharp rise in entropy production. Such an increase is not predicted for uniform flow distribution across parallel channels, making maldistributed flow a thermodynamically favored state over equally distributed flow. Maldistributed flow corresponds to the highest entropy production rate compared to other steady two-phase flow distributions for similar system constraints. Such flow behavior also exists in non-identical channels, wherein moderately non-uniform flow distributions could be predicted. However, in practice, the flow distribution is more significantly non-uniform since it is thermodynamically favored and corresponds to a higher entropy production rate.

Entropy analysis is often omitted from the modeling and performance prediction of systems with multiphase flow and liquid-vapor phase change. This study shows how entropic considerations provide an additional perspective to understand and predict the behavior of nonlinear systems with several possible outcomes. This study analyzes stable and unstable flow distribution in two thermally isolated parallel channels and is therefore unsuitable for application to parallel channels with significant thermal coupling, such as a system of parallel channels constructed on a metallic substrate. Nevertheless, the principle of maximum entropy production may be extended to analyzing a larger system of parallel channels experiencing heating and multiphase flow or even thermally coupled channels.

7 ACKNOWLEDGMENTS

- 397 The work was supported by the National Science Foundation's Division of Chemical,
- 398 Bioengineering, Environmental, and Transport Systems in the Directorate for Engineering under
- 399 Grant No. 1944323.

8 References

400

413

414

415

416

417

418

- T. Aka and S. Narayan, "Transient Behavior and Maldistribution of Two-Phase Flow in Parallel Channels," *IEEE Transactions Components Packaging Manufacturing Technology*, vol. 12, no. 2, pp. 270–279, 2022.
- 404 [2] E. Manavela Chiapero, M. Fernandino, and C. A. Dorao, "Numerical analysis of pressure drop oscillations in parallel channels," *International Journal of Multiphase*406 *Flow*, vol. 56, pp. 15–24, 2013.
- 407 [3] T. Van Oevelen, J. A. Weibel, and S. V. Garimella, "Predicting two-phase flow distribution and stability in systems with many parallel heated channels,"

 409 International Journal of Heat and Mass Transfer, vol. 107, pp. 557–571, 2017.
- 410 [4] C. Guermonprez, S. Michelin, and C. N. Baroud, "Flow distribution in parallel microfluidic networks and its effect on concentration gradient," *Biomicrofluidics*, vol. 9, no. 5, Sep. 2015.
 - [5] B. H. Lim, E. H. Majlan, W. R. W. Daud, M. I. Rosli, and T. Husaini, "Numerical analysis of flow distribution behavior in a proton exchange membrane fuel cell," *Heliyon*, vol. 4, p. 845, 2018.
 - [6] J. C. Pacio and C. A. Dorao, "A study of the effect of flow maldistribution on heat transfer performance in evaporators," *Nuclear Engineering and Design*, vol. 240, no. 11, pp. 3868–3877, Nov. 2010.
- T. Zhang, J. T. Wen, A. Julius, Y. Peles, and M. K. Jensen, "Stability analysis and maldistribution control of two-phase flow in parallel evaporating channels,"

421		International Journal of Heat and Mass Transfer, vol. 54, no. 25–26, pp. 5298–5305,
422		2011.
423	[8]	G. Patankar and T. R. Salamon, "Maldistribution of Two-Phase Flow in Parallel
424		Channel Heat Sinks: Effects of Thermal Connection between Channels,"
425		Proceedings of the 17th InterSociety Conference on Thermal and Thermomechanical
426		Phenomena in Electronic Systems, ITherm 2018, pp. 653–663, 2018.
427	[9]	U. Minzer, D. Barnea, and Y. Taitel, "Evaporation in parallel pipes - Splitting
428		characteristics," International Journal of Multiphase Flow, vol. 30, no. 7-8 SPEC.
429		ISS., pp. 763–777, 2004.
430	[10]	Y. Taitel, U. Minzer, and D. Barnea, "A control procedure for the elimination of mal
431		flow rate distribution in evaporating flow in parallel pipes," Solar Energy, vol. 82,
432		no. 4, pp. 329–335, 2008.
433	[11]	V. Manoj Siva, A. Pattamatta, and S. K. Das, "Effect of flow maldistribution on the
434		thermal performance of parallel microchannel cooling systems," International
435		Journal of Heat and Mass Transfer, vol. 73, pp. 424-428, 2014.
436	[12]	U. Minzer, D. Barnea, and Y. Taitel, "Flow rate distribution in evaporating parallel
437		pipes-modeling and experimental," Chemical Engineering Science, vol. 61, no. 22,
438		pp. 7249–7259, 2006.
439	[13]	P. Yang, K. Tian, Z. Tang, N. Li, M. Zeng, and Q. Wang, "Flow Distribution and
440		Heat Transfer Performance of Two-Phase Flow in Parallel Channels with Different
441		Cross Section," Chemical Engineering Transactions, vol. 94, pp. 703–708, 2022.

142	[14]	S. Natan, D. Barnea, and Y. Taitel, "Direct steam generation in parallel pipes,"
143		International Journal of Multiphase Flow, vol. 29, no. 11, pp. 1669–1683, 2003.

- [15] B. Sun, H. Chang, and Y. L. Zhou, "Flow regime recognition and dynamic characteristics analysis of air-water flow in horizontal channel under nonlinear oscillation based on multiscale entropy," *Entropy*, vol. 21, no. 7, Jul. 2019.
- [16] J. C. Ordóñez and A. Bejan, "Entropy generation minimization in parallel-plates counterflow heat exchangers," *International Journal of Energy Research*, vol. 24, no. 10, pp. 843–864, Aug. 2000.
- [17] O. S. Ezeora and O. Ezeora, "Purdue e-Pubs Entropy Generation Analysis and Optimum Tube Length of Two-Phase Flow Evaporator Tube Entropy Generation Analysis and Optimum Tube Length of Two-Phase Flow Evaporator Tube."

 [Online]. Available: http://docs.lib.purdue.edu/iracc/961
- [18] M. N. Hossain and K. Ghosh, "Entropy generation minimization for boiling flow inside evaporator tube with R32 and R410A refrigerants: a comparison of different two-phase flow models," *Journal of Thermal Science and Engineering Applications*, pp. 1–38, Feb. 2023.
- [19] L. S. Maganti and P. Dhar, "Consequences of flow configuration and nanofluid transport on entropy generation in parallel microchannel cooling systems," *International Journal of Heat and Mass Transfer*, vol. 109, pp. 555–563, 2017.

461	[20]	P. Županović, D. Juretić, and S.	Botrić, "Kirchhot	ff's loop law and the	maximum		
462		entropy production principle," F	Physical review.	E, Statistical physics	, plasmas,		
463		fluids, and related interdisciplinar	ry topics, vol. 70,	no. 5, p. 5, 2004.			
464	[21]	N. Giannetti, M. A. B. Redo, K. S	Saito, and H. Yosl	nimura, "Variational f	ormulation		
465		of stationary two-phase flow dis	tribution," Case S	Studies in Thermal Er	ngineering,		
466		vol. 26, Aug. 2021.					
467	[22]	A. Sahoo and R. Nandkeolyar, '	Entropy generation	on and dissipative he	at transfer		
468		analysis of mixed convective hydro	omagnetic flow of	a Casson nanofluid w	ith thermal		
469		radiation and Hall current," Sci Re	<i>ep</i> , vol. 11, no. 1, 2	Dec. 2021.			
470	[23]	D. B. Pengra, "Notes on Data Analysis and Experimental Uncertainty." Accessed:					
471		Oct. 10,	2023.	[Online].	Available:		
472		https://courses.washington.edu/ph	ys431/uncertainty	_notes.pdf			
473	[24]	T. Aka, "Uncertainty_Prop." MA	ΓLAB Central Fil	e Exchange, Aug. 12,	2023.		
474	[25]	I. Novikova, "Analysis of exper-	rimental data," 2	008. Accessed: Oct.	10, 2023.		
475		[Online]. Available: https://course	es.washington.edu	/phys431/uncertainty_	notes.pdf		
476							